IOPscience iopscience.iop.org

Home Search Collections Journals About Contact us My IOPscience

Harmonic measure around a linearly self-similar tree

This article has been downloaded from IOPscience. Please scroll down to see the full text article.

1992 J. Phys. A: Math. Gen. 25 1781

(http://iopscience.iop.org/0305-4470/25/7/020)

View the table of contents for this issue, or go to the journal homepage for more

Download details:
IP Address: 171.66.16.62
The article was downloaded on 01/06/2010 at 18:14

Please note that terms and conditions apply.

J. Phys. A: Math. Gen. **25** (1992) 1781–1797. Printed in the UK

Harmonic measure around a linearly self-similar tree*

Carl J G Evertsz†§ and Benoit B Mandelbrot‡

† Applied Physics Department, Yale University, Box 2155, Yale Station, New Haven, CT 06520, USA

‡ Physics Department, IBM T J Watson Research Center, Yorktown Heights, NY 10598, and Mathematics Department, Yale University, New Haven, CT 06520, USA

Received 24 July 1991, in final form 25 November 1991

Abstract. We use the concept of random multiplicative processes to help describe and understand the distribution of the harmonic measure on growing fractal boundaries. The Laplacian potential around a linearly self-similar square Koch tree is studied in detail. The multiplicative nature of this potential, and the consequent multifractality of the harmonic measure are discussed. On prefractal stages, the density $d\mu$ of the harmonic measure and the corresponding Hölder $\alpha = -\ln d\mu$ are well defined along the boundary, except in the folds where the tangent is undefined. A regularization scheme is introduced to eliminate these local effects. We then consider the probability distributions $P(\alpha)\,d\alpha$ of successive stages, and discuss their collapse into an $f(\alpha)$ curve. Both the left- and right-hand sides of this curve show good convergence. Other studies indicate that, for DLA, the right-hand tail does not converge. A brief comparison is made between the multifractality of these two cases.

1. Introduction

This paper investigates the Laplace potential around a linearly self-similar Koch curve $\boldsymbol{K}$, which is the limit of the well known recursive Koch construction illustrated in figure 1. The limit boundary subdivides into trees, each of which is linearly ('exactly') self-similar [1, 2], with the fractal dimension $D = \log 5/\log 3 \approx 1.465$.

As intended, this boundary bears a general resemblance to a cylindrical diffusion-limited aggregate (DLA) [3]. More precisely, the successive prefractal approximations of $\boldsymbol{K}$ bear a resemblance to scaled-down pictures of successive stages of growth of DLA. However, one must keep in mind that $\boldsymbol{K}$ is very much simpler than DLA, because DLA clusters *are not* linearly self-similar, even in a statistical sense. Therefore, we *do not* expect our observations to be descriptive of DLA, but only to provide a helpful background against which the complexities and the specificity of the properties of DLA can be assessed. Of course, the dimension $D = 1.465$ is far below the value $D = 1.7$ [3, 4] for DLA, but this difference is not significant for our purposes.

Much of the work to be reported concerns the Laplacian potential around $\boldsymbol{K}$, and its normalized harmonic measure, that is, its normalized gradient. Here, the natural tool is the concept of the multifractal [5–7], including a function ordinarily denoted by $f(\alpha)$. There is a naive belief that multifractal analysis reduces to the evaluation of $f(\alpha)$, but we believe that knowing $f(\alpha)$ is not enough. A more detailed knowledge of

* Illustrated by François Normant, Applied Physics Department, Yale University, Box 2155 Yale Station, New Haven, CT 06520, USA.

§ Present address: Institut für Dynamische Systeme, Universität Bremen, Postfach 330 440, D-2800 Bremen 33, Federal Republic of Germany.

0305-4470/92/071781+17$04.50 © 1992 IOP Publishing Ltd

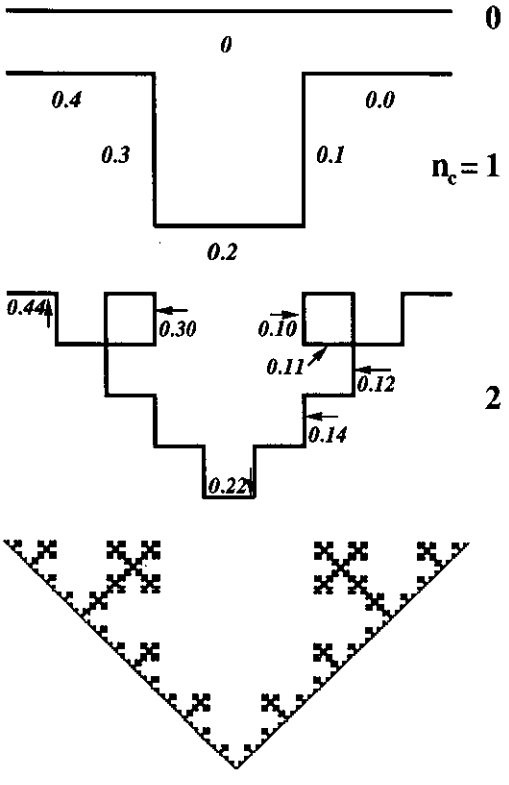

Figure 1. The geometric cascade generating the square Koch tree. Each line segment has a unique base 5 coding. When applicable, the orientation of the digits are taken such that segment 0 has larger harmonic measure than segment 4. For example, in an orientation induced on tracing the curve, the segment coded 0.30 would have been 0.34. A cavity is coded by its presegment. Thus, cavity 0.1 is the structure formed by all the segments whose expansions start with either 0.11 . . . , 0.12 . . . or 0.13 . . . . The limit set has fractal dimension $D = \ln 5/\ln 3$.

the geometry is necessary. In particular, a basic fact is that the only fractals one understands thoroughly are those obtained by recursive schemes; similarly, the only multifractals one understands really well are those obtained by a multiplicative 'cascade process', of a kind L F Richardson has postulated in turbulence [1]. As is the case for every formalism, the formalism of multifractals applies in a wider but ill-defined context; a central issue is how close a multifractal is to being multiplicative.

The non-random binomial and multinomial measures on [0, 1] are examples of exact multiplicative measures [8] which have been studied long ago by mathematicians of the school of A S Besicovitch. The basic step is to subdivide [0, 1] into b intervals, then repeat the subdivision recursively, each step yielding an increasingly fine-grained measure. Random generalizations have been investigated by one of us (BBM) around 1970 [5]. In earlier studies [9, 10] we have found that it is very fruitful to consider the harmonic measure of DLA as being multiplicative, but we had no direct test of the validity of this assumption. This motivated us to investigate to what extent it is also useful to consider the harmonic measure μ around our Koch trees as multiplicative. Numerical and analytical studies [11-13] of the harmonic measure on linearly self-similar trees show that this measure is a restricted multifractal [5-7, 14, 15], in the

sense that the distribution of α is described by a curve $f(\alpha)$ shaped like the symbol $\cap$. A connection between multiplicative processes and this restricted form of multifractality, which is characteristic of the harmonic measure on linearly self-similar sets, has been assumed and used in [9, 10, 13, 16, 17].

In demonstrating the existence of an underlying multiplicative process, the present paper goes beyond an evaluation of $f(\alpha)$, and investigates the whole Laplacian potential field around the square Koch tree $\boldsymbol{K}$. Here, a counterpart to the recursive subdivision of [0, 1] is the recursive cascade construction illustrated in figure 1. We follow the potential itself and the harmonic measure as our Koch prefractal tree is progressively refined by the addition of increasing numbers of progressively smaller 'bays'. The move from the potential to the harmonic measure involves many surprisingly subtle points, which we felt deserved to be faced squarely, and are discussed in later sections. However, a bit of 'hand waving' suffices to describe a few basic facts, and to support the idea that the measure is approximately multiplicative.

Another issue we have dealt with concerns the definition of the harmonic measure that is to be used in the description of its multifractality. In theory, the density of the harmonic measure is proportional to the gradient of the continuum Laplacian potential on the boundary. However, following the pioneering use of the Laplacian in this context [18, 19], most numerical and analytical works on DLA have dealt with a spatially discrete Laplacian potential. Setting the potential at the boundary to $\phi = 0$, these works approximate the non-normalized harmonic measure by the potential at the nearest neighbours of the boundary. The resulting 'site probability' is used to estimate the harmonic measure of that small portion of the cluster's boundary which is nearest to the site and has a length about the size of the lattice constant.

In the context of the discrete potential, these site probabilities seem natural, but in our context they demand closer examination. While discretization is a necessity for numerical analysis, the quantities used to characterize the harmonic measure on a boundary should not depend on the lattice constant. Unfortunately, the site probabilities do show such dependence, and therefore are inappropriate for an intrinsic description. The alternative method we use starts with the density of the harmonic measure. On-lattice DLA [3, 18] establishes an artificial coupling between the particle size and the lattice constant associated with the discrete Laplacian. From that viewpoint, this delicate issue that we raise may seem irrelevant. It is, however, crucial for the description and study of the harmonic measure on off-off-lattice DLA [20, 21].

2. Visualization of the multiplicative cascade

The method of zebra rendering is described in the caption of figure 2. The left-hand side of figure 2(*d*) shows a zebra rendering of the Laplacian potential field around the square Koch tree $\boldsymbol{K}$. The hierarchical structure of the fjords in this fractal curve is clearly visible. References [9, 20] show similar zebra renderings of the potential around DLA boundaries.

Let us inspect figures 2(*a*)-(*d*) carefully. One first notes that the *larger-scale* features of the potential field, that is, the features defined by a certain level of the geometrical cascade, are left virtually untouched by the geometric details added by the next step of the cascade. That is, the stacks of zebra stripes are to a large degree unchanged when a main fjord is perturbed by subfjords half the previous size. This fact is in full agreement with the Carleson-Jones method for estimating the extremal length with

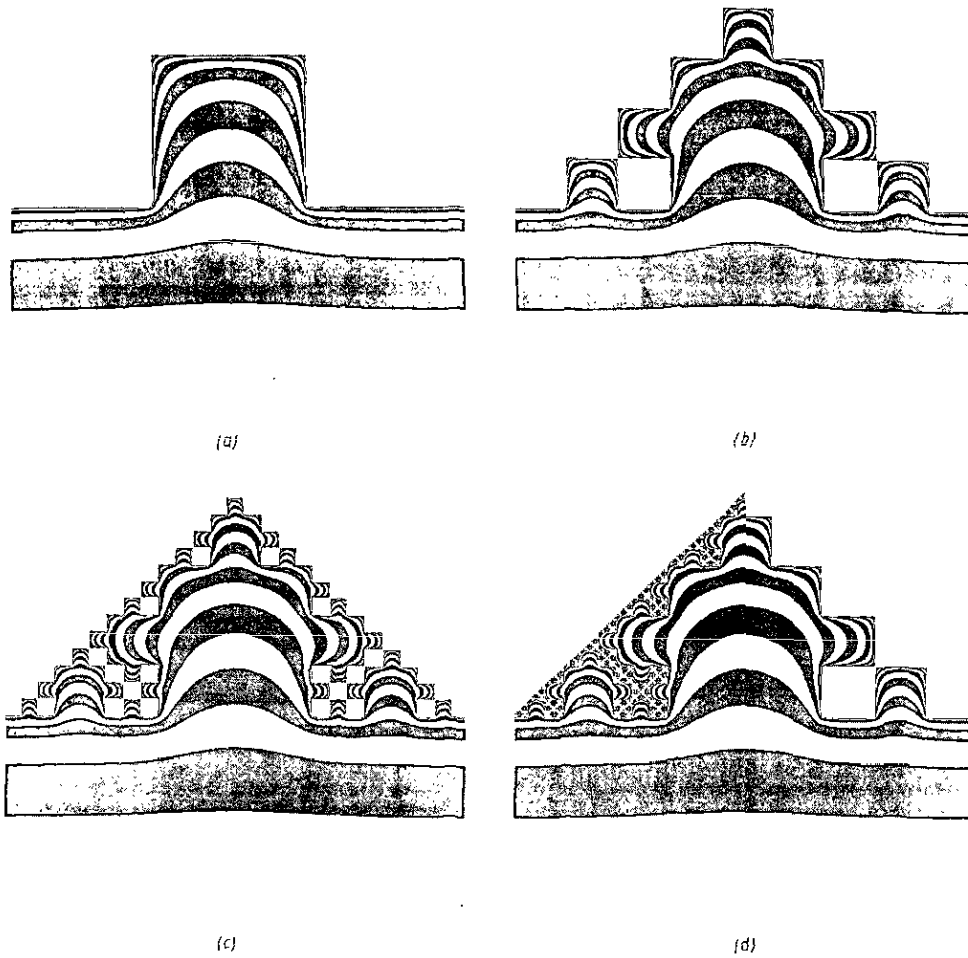

Figure 2. Zebra rendering of the Laplacian potential around different prefractal stages of the self-similar square Koch tree. The logarithm of the potential is linearly binned in black and white stripes. Each stripe is a factor ≈ 2 drop in the potential. The geometry has been turned upside down to emphasize the growing tree. Geometric detail is added by the following step in the geometric cascade, but it will leave the larger scales of the zebra pattern untouched. The result is a local addition of stripes, which is equivalent to a local multiplication of the measure. Thus this is a visualization of the multiplicative process enforced on the Laplacian potential field by a self-similar boundary. See also figure 3. The left half of d is $n_c = 5$, the right half is $n_c = 1$.

the help of discs [22, 23]. Thus, the number of zebra stripes from a point outside the set to the entrance of fjord 0.1 (as depicted in figure 1) remains approximately the same before and after the addition of fjord 0.1. In terms of the potential field around the boundary, the addition of fjord 0.1 'grafts' an extra branch onto an already existing tree of earlier-generation zebra stripes.

2.1. The complementary Laplacian tree

Leaving the prefractals of $\boldsymbol{K}$ aside for a moment, let us examine how the zebra patterns change as one moves along figures 2(a)-(c). They reveal a new complementary

Laplacian cascade. It is so regular that, knowing the shapes of stages *a* and *b*, one could almost guess the shape of stage *c*.

At each new stage of this complementary cascade, the two-dimensional zebra-rendered surface of the Laplacian tree is enlarged. One observes additional zebra stripes that were present in the preceding stage, but were so close together that our illustration could not separate them. This accretion of new stripes is additive in terms of the zebras based on the logarithm of the potential, hence is multiplicative in terms of the potential itself. The total number of zebra stripes needed to reach a newly added smallest Laplacian branch depends on the location of that branch. For example, inspect one of the smallest most recently added fjords in stage *c*. The unnormalized Hölder $\alpha = -\ln \mu$ is proportional to the number N of stripes between this fjord and the bottom of the figure. Therefore, the total harmonic measure on the surface of this fjord is proportional to $\exp(-N)$, where the constant of proportionality depends upon the width of the zebra stripes used in rendering.

The multiplicative process appears in its most elementary form in the subset of fjords whose expansion, explained in the caption of figure 1, only involves the digits 1, 2 and 3. If the Hölder at the entrance of 0 in figure 1 is denoted by $\alpha(0)$, count the extra number of stripes V in figure 2(*c*) needed to reach these entrances: $\alpha(0.1) = \alpha(0.3) \approx \alpha(0)+4$ and $\alpha(0.2) \approx \alpha(0)+6$. Similarly, $\alpha(0.22) \approx \alpha(0)+6+6$ and $\alpha(0.12) \approx \alpha(0)+4+6$. This extra number of stripes $V \approx -\log M$, where M is the multiplication factor in the potential.

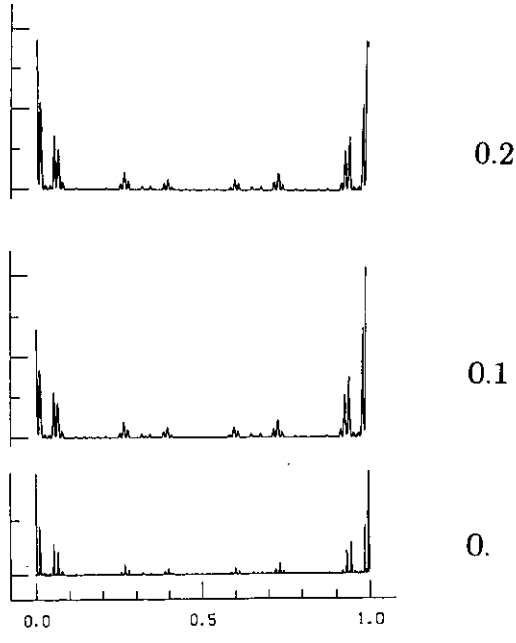

Figure 3. A different illustration of the multiplicative process discussed in figure 2. From top to bottom one finds, stretched out and mapped to [0, 1], the boundaries of the fjords 0.2, 0.1 and 0, with their harmonic densities normalized to 1. The normalized densities on 0 and 0.2 are nearly identical, while 0.1 is a bit skew. This is due to the fact that the potential is decreasing in going from segment 0.10 to 0.14. This skewness is smooth compared to the irregularities in the basic form (0) of the density; it adds an extra touch of complication to the multiplicative process, compared to a simple multinomial multifractal.

The subset of fjords characterized by the digits 1, 2 and 3 clearly illustrates two important properties. First, the Laplacian potential is multiplicative, hence the same is true of the harmonic measure. Second, moving away from the potential to the Hölder $-\log \mu$ transforms the multiplicative process into addition of random variables. The result is that one can use the limit theorems for sums of random variables, a step that is essential in the probabilistic theory of multifractals [5, 10]. In the case of our potential around $\boldsymbol{K}$, the random variable $V = -\log M$ can take the values $V = 6$ and $V = 4$ with the respective probabilities $\frac{1}{3}$ and $\frac{2}{3}$. Such a bounded addend is known to give rise to a 'restricted multifractal' [2].

The fjords that also contain the digits 0 and 4 in their expansion are discussed in section 5.

2.2. Self-similarity of the harmonic measure

In the case of $\boldsymbol{K}$, the self-similarity of the harmonic measure is due to the self-similarity of the boundary and the scale invariance of the Laplacian. Certain connected subsets of the geometry are replicated within themselves on smaller scales. For example, consider fjords 0.1 and 0.2 in figure 1, together with their smaller-scale decorations; they are scaled-down versions of the main fjord 0. The scale invariance of the Laplacian is discussed in detail in section 3; it implies that the harmonic measure is approximately the same in each of these replicas, except for a multiplicative factor due to screening. Figure 3 illustrates this effect by stretching out the boundaries of the main fjord 0 and of the subfjords 0.1 and 0.2, together with the density-Hölders, and by mapping them on the unit interval. The resemblance is evident, as expected.

3. Scale invariance of the Laplace equation

Consider the simple boundary shown in figure 4. The two separate square-shaped cavities B and B' in the lower-half plane are related by a translation (a, b) and a scale transformation $B' = \lambda B$. Let $\phi(x, y)$ be the solution of the Laplace equation

$$\nabla^2 \phi = \left(\frac{\partial^2}{\partial x^2} + \frac{\partial^2}{\partial y^2} \right) \phi = 0 \tag{1}$$

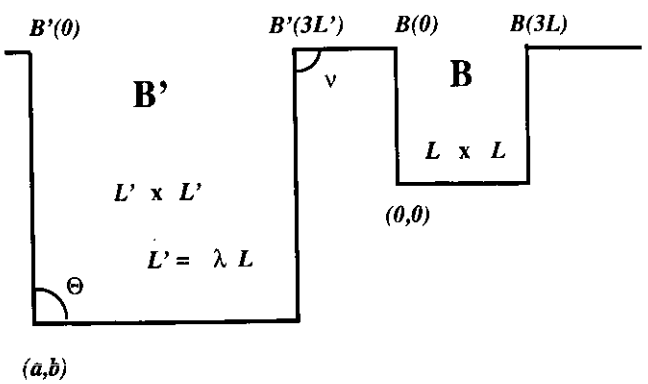

Figure 4. A simple boundary consisting of two separated rectangular fjords, B and B', which are identical modulo a scale transformation $\lambda = 2$. The Laplacian is solved between the boundary, which is set at potential 0 and a horizontal line high above, which is kept at potential 1 (see also figure 5).

with boundary conditions $\phi(B)=0$, and $\phi=1$ along a boundary far away from $\boldsymbol{K}$. Using the coordinate transformation $(x', y') \mapsto (x, y) = (x'-a, y'-b)/\lambda$, we see that $\phi'(x', y') \equiv c\phi((x'-a)/\lambda, (y'-b)/\lambda)$ solves the Laplace equation with boundary condition $\phi'(B')=0$. The constant c depends on the boundary conditions outside the cavities, and we will argue below that in this case it equals λ. It follows that the potentials ϕ and ϕ', corresponding to two boundaries B and B' which differ by transformation of scale, are identical modulo a factor and a similarity transformation of spatial scales. This is immediately apparent from the zebra rendering of the potential field in figure 5, where $-\log\phi$ has been binned in black and white. The potential is rendered by superimposing a 'foggy' background that becomes progressively darker as the potential decreases.

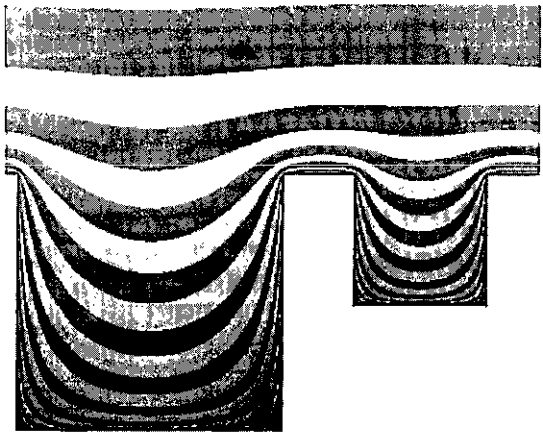

Figure 5. Zebra rendering of the Laplacian potential in the upper part of the boundary in figure 4. The zebra stripes result from a linear binning of $-\log\phi$, where ϕ is the potential estimated numerically on a square lattice with $L=100$.

4. Density of the harmonic measure

We begin with a remark concerning the notation we use for the harmonic measure. The boundary of our cluster is one-dimensional, hence it can be parametrized by a real number t in the interval $[0, 1]$. The measure of the piece of B parametrized by the interval $[0, t]$ can be denoted by $\mu(t)$. Hence, given a piece of B parametrized by dt, its measure can be denoted by $d\mu(t)$. A segment $[t', t'']$ of the boundary carries the measure $\int_{t'}^{t''} d\mu(t) = \mu([t', t''])$. This notation is equally meaningful for the prefractal approximates of $\boldsymbol{K}$, and for the limit $\boldsymbol{K}$. For the former, the measure is differentiable except for isolated singularities. For the latter, the measure is nowhere differentiable.

Now we return to our argument. Let the boundary of the cavities B and B' be parametrized by arc length, starting from the upper left corner and moving towards the upper right one, i.e. $B=B(t)$, $t=[1, 3L]$ and $B'=B'(t')$, $t'=[1, \lambda 3L]$, where L and L' are the sizes of the respective cavities' edges. At boundary element $B(t)$ the

harmonic measure $d\mu(t)$ is proportional to the absolute value of the gradient of the Laplacian potential, which is perpendicular to the boundary, i.e. $d\mu(t) \sim E(t)$. From the scale invariance of the Laplacian, $E'(t') = (c/\lambda)E(t'/\lambda)$. By integrating the density $d\mu(t) \sim E(t)$ of the harmonic measure along the boundary, we find that the harmonic measures of the two cavities in figure 4 differ by a factor c, and satisfy $\mu(B') = c\mu(B)$.

Now the probability for the Brownian point to enter B' is λ times larger than the probability for it to enter B. On the other hand, the probability for the Brownian point to stick somewhere on B', conditional to its entering B', is the same for both B' and B. So $\mu(B') = \lambda\mu(B)$ [24]; this shows $c = \lambda$.

Thus, the densities of the harmonic measure in B and B' are identical, to a spatial scale transformation; this shows that $d\mu'(t') = d\mu(t'/\lambda)$.

4.1. Static local singularities

It is well known that the density $d\mu$ has power law singularities at the *folds* $B'(0)$, $B'(L')$, $B'(2L')$ and $B'(3L')$. In a region s around a tip such as $B'(0)$, where the internal angle is $\vartheta(=\pi/2)$, the harmonic measure scales like $s^{\tilde{\alpha}}$, with $\tilde{\alpha} = \pi/(2\pi - \vartheta)$. At $B'(0)$ and $B'(3L')$, the density is ∞ ($\tilde{\alpha} < 1$), while at the other two folds it is 0 ($\tilde{\alpha} > 1$). The exponent $\tilde{\alpha}$ is called the local Hölder.

These singularities are static, because they are not related to a development of the boundary, and local, because only the internal angle is relevant, while the size of the fold is irrelevant; a fold in an otherwise differentiable boundary, however small, gives rise to a local singularity in its harmonic measure.

In the study of the self-similarity of the harmonic measure on a growing fractal boundary, in general, one is not interested in such local singularities. Of interest are singularities in the harmonic measure which are due to the interaction between a *growing* (random) fractal boundary and the Laplacian potential.

4.2. Dynamic singularities and regularization

If, instead of K, we had examined a DLA boundary, its singularities would have shown up dynamically, i.e. as functions of the number of atoms in the cluster. However, in order to clearly detect these singularities, the measure has to first be *regularized* to eliminate the divergences in its density due to local singularities.

Our regularization scheme is as follows. Denote the harmonic measure of a segment $B([t_0, t_1])$ by $\mu(t_0, t_1)$. Given $\varepsilon > 0$, the ε-regularized harmonic density at boundary point $B(t)$ is defined as

$$d\mu_\varepsilon(t) = \frac{1}{\varepsilon}\mu\left(t - \frac{\varepsilon}{2}, t + \frac{\varepsilon}{2}\right). \tag{2}$$

Thus, the regularized density $d\mu(\varepsilon)$ is such that the local Hölder

$$\alpha(t) = \lim_{x \to 0} \frac{\ln \int_t^{t+x} d\mu_\varepsilon(t)}{\ln x} \tag{3}$$

satisfies $\alpha(t) = 1$ everywhere (see appendix 1) and is normalized so that $\int d\mu(t) = 1$. *The only singularities that can arise in the regularized measure are due to the development*

of the structure as L increases. For fixed regularization parameter, the singularity at a given point, e.g. at the tip $B(0)$, appears in the behaviour of the harmonic density $d\mu_\varepsilon(0) \sim L^{-\alpha}$ as a function of the size L of the structure. Appendix 2 describes a simple example.

Let $P(\alpha)\,d\alpha$ denote the probability that, given a randomly picked point t on the boundary, the density-Hölder $\alpha(t) = -\log d\mu(t)$ lies between α and $\alpha + d\alpha$. From the fact that the densities on both cavities B and B' are the same, i.e. $d\mu'(t') = d\mu(t'/\lambda)$, an important consequence follows: *the contributions of B and B' to the probability density $P(\alpha)\,d\alpha$ are identical.* Thus, $P_{tot}(\alpha) = P_B(\alpha) + P'_{B'}(\alpha) + P_{rest}(\alpha)$, with $P'_{B'}(\alpha') = P_B(\alpha')$. (See appendix 3 for proof.)

Denote by $N(\alpha, \alpha + d\alpha)$ the number of sites with Hölders between α and $\alpha + d\alpha$. Figure 6 shows numerical estimates for $\ln N_B(\alpha, \alpha + d\alpha)$, $\ln N_{B'}(\alpha, \alpha + d\alpha)$, and $\ln N_{tot}(\alpha, \alpha + d\alpha)$ (circles), and the sum $\ln(N_B + N_{B'})$ (squares). Denote by ϕ_i the solution of the discrete Laplace equation at nearest neighbour i. Then taking the lattice constant $\delta = 1$, the quantities $d\mu(i) = \phi_i / \Sigma_j \phi_j$, where the sum runs over the total boundary, are estimates of the harmonic density at i. The αs in figure 6 are density-Hölders $\alpha = -\log(d\mu(i))$ regularized on a lattice, with $\varepsilon = \delta$. The numerical estimates for $\mu(B)$ and $\mu(B')$ are 0.20 and 0.36, respectively. The ratio between the two is thus close to the theoretical result $\mu(B')/\mu(B) = \lambda = 2$. The same ratio is found between N_B and $N_{B'}$, except for deviations at the tails, which are affected by the singularities at the folds; these singularities are better articulated in B' than in B. The bump to the left of the graph of $\ln N_{tot}$ (circles) is due to the horizontal unscreened lines connecting the two cavities; it is of course absent from the graph $\ln(N_B + N_{B'})$ (squares).

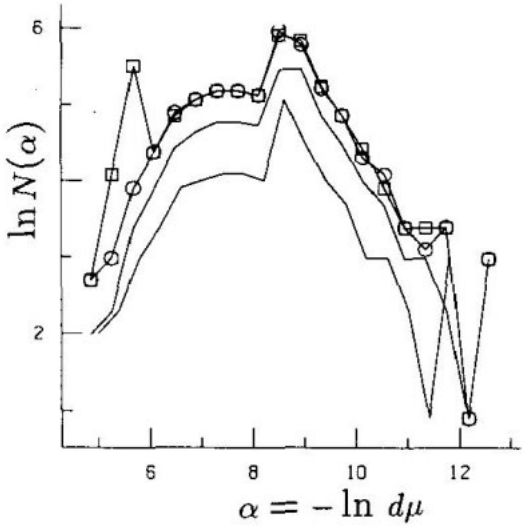

Figure 6. The curve marked with squares is the logarithm of the number density $\ln N(\alpha)$ of density-Hölders $\alpha = -\ln d\mu$, of the total boundary in figure 4. The bottom curve is the contribution N_B from the small fjord B, and the next higher curve is $N_{B'}$. These curves are identical modulo $\lambda = 2$, i.e. $N_{B'} = 2N_B$. This illustrates that two fjords which are identical modulo a scale transformation λ have the same contribution, modulo a weighing factor, to the $f(\alpha)$ curve. The curve marked in circles is the addition of these contributions. The difference between the circles and the squares is the contribution of the horizontal pieces joining the cavities.

5. Size and nesting level of a fjord

In the construction of $\boldsymbol{K}$ that is shown in figure 1 all fjords of a certain size are added at the same time, i.e. they belong to the same (cascade) generation. This relates the age of a fjord, defined by the cascade generation number, and its size. There is, however, an alternative hierarchical categorization based on the nesting of fjords within fjords. The related *nesting* number n_s is the number of higher-generation fjords the potential field has to cross in coming from the outside towards a subfjord, plus 1. For a fjord with expansion $0, a_1 a_2 \ldots a_k$, with $a_i = 0, 1, 2, 3, 4$, the cascade generation number is $n_c = k$, and the nesting number n_s is equal to 1 plus the number of digits 1, 2 or 3.

The multiplicative process appears in its most elementary form in the subset of fjords having only digits 1, 2 and 3. Such fjords satisfy $n_c = n_s$. Thus, the absolute value of the base 3 logarithm of the size 3^{-n_c} of a subfjord is equal to n_s, making it equal to the number of stages in the multiplicative process. Thus, the alternative Hölder defined by $\alpha = -\ln \mathrm{d}\mu / \ln(\text{size})$ [5–7], is proportional to the average number of stripes per subfjord through which the electric field line passes in figure 7. Note that for stripe counting to make sense one should avoid boundary details such as the folds, which interfere with the density, but are irrelevant. Therefore, stripe counting is started at some fixed positive distance from the boundary; this distance must be smaller than the smallest details in the boundary, but must not be too small.

Clearly, the average number of stripes α is largest for the fjord with expansion $0.22\ldots2$ and smallest for the fjords $0.11\ldots1$ and $0.33\ldots3$. The αs follow a skew binomial distribution ranging between these two extremes. The smallest harmonic measure on a linearly self-similar curve will always be at the bottom of one of the fjords with the maximum nesting number n_s. The reason is that after the maximum

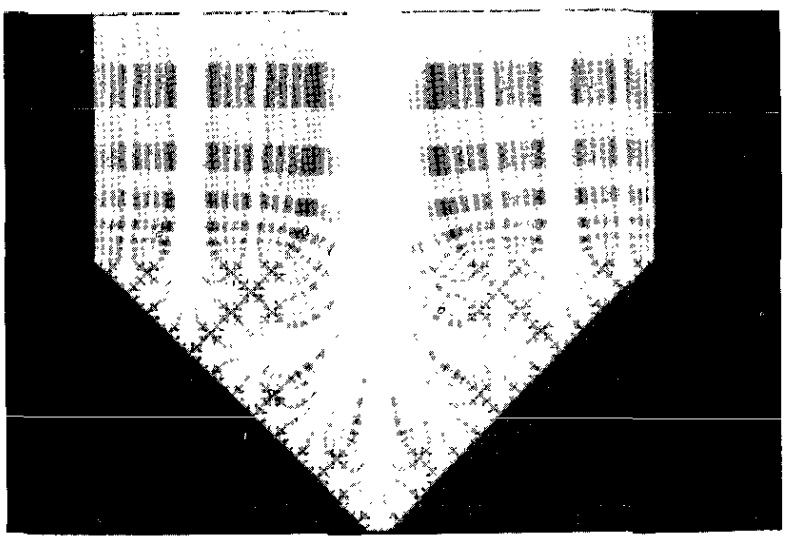

Figure 7. Electric field lines around the square Koch tree, *also called lines of force or* current lines. Repulsive massless charged particle are homogeneously distributed along the surface of the square Koch tree, and then released. This picture is a rendering of the logarithm of the density of particles passing through a point on their way to infinity for an $n_c = 5$ prefractal square Koch tree. This is not the customary representation; however, we have found it more useful in illuminating the structure of the problem. It has been especially powerful in the case of current lines in DLA [20].

amount of zebra stripes added in a region of the boundary has been modified by the addition of a fjord, it always takes the same value, because the added fjords have the same shape modulo a scale transformation. For $\boldsymbol{K}$, this smallest harmonic measure is always at the bottom of the oldest fjord 0, namely in $0.22\ldots2$ (a notion of age is defined in section 7).

When a fjord's expansion also involves the digits 0 and 4, the multiplicative mechanism is less apparent. The logarithm of such a fjord's size is not related to n_s, which in the above scheme was the number of multiplicative states. At cascade generation n_c there are

$$2^{n_c-k}3^{k-1}\binom{n_c}{k}$$

fjords of size 3^{-n_c} with $n_s = k$. Yet, the conventionally normalized Hölder ($1/\ln(\text{size}) \sim n_c^{-1}$) still makes sense for $n_s \neq n_c$. This can be illustrated with the extreme cases where $n_s = 1$. There are 2^{n_c-1} such smallest cavities. All are located in the top row, and connect directly with the empty upper-half plane. From the study of the situation in figure 4, it follows that (if the external circumstances were the same) the harmonic density in such a cavity would be the same as in cavity 0 in the prefractal stage $n_c = 1$ of $\boldsymbol{K}$. Thus, the normalized density-Hölders would converge to 0. However, the external circumstances are not the same. The $n_s = 1$ cavities move closer—by an amount of 3^{-n_c}—to the power law singularities in the folds in the envelope of the fractal boundary. Therefore, the normalized density-Hölders converge to the local Hölder $\approx \alpha = \frac{2}{3}$ [25], corresponding to the internal angle $\pi/2$ of these folds.

A similar coexistence of many different levels of fjord nesting within one growth stage (i.e. cascade generation) is also present in DLA.

6. The limit distribution $f(\alpha)$ for the Hölder α on a square Koch tree

Given a structure like the prefractals in figure 1, the calculation of the harmonic measure through the Laplacian requires a metric. The measure itself is independent of the metric. Its (regularized) density, however, does depend on the metric, and thus on the size of the object.

The development of the boundary, which we expect gives rise to a multiplicative process, necessarily involves either (i) the creation of a new structure on larger scales, or (ii) the creation of a new structure on smaller scales, or (iii) both. Knowledge of both the shapes and sizes of different stages in the development of a boundary are therefore necessary for a quantitative analysis of the multifractal properties of its harmonic measure.

In the case of DLA, the different stages and their sizes are linked through growth. In the square Koch tree $\boldsymbol{K}$, the geometric cascade could have been interpreted in either of the three ways that have been mentioned. Since we want the point of view closest to growing DLA boundaries, we interpret the cascade as growth, i.e. the creation of structure on larger scales.

Thus, the horizontal sizes of the nth ($=n_c$th) stages of the cascade, as shown in figures 2(a)-(c), scale like 3^n. For convenience, we will take this size to be $L(n) = 3^n$. In all the cases shown in figure 2, the lattice used in the numerical estimate of the electrostatic potential was $729 \times 700 = 3^6 \times 700$. The absolute size of the lattice constant was therefore $\delta(n) = 3^n/3^6 = 3^{n-6}$, $n = 1, \ldots, 5$.

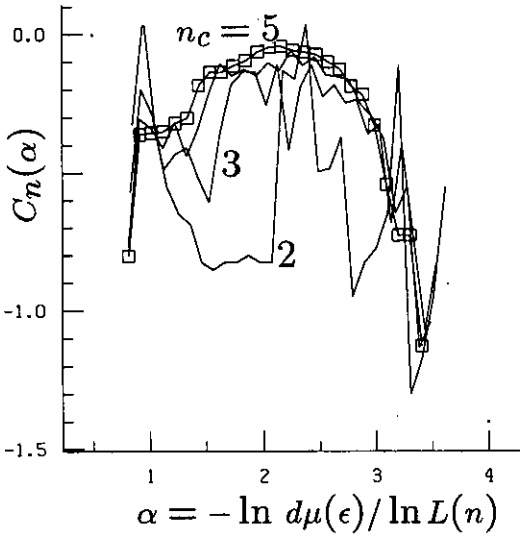

Figure 8. Cramèr plot, $C_n(\alpha) = \ln_{L(n)} P_n(\alpha)$ versus α, of the probability densities $P_n(\alpha)\,d\alpha$ of the Hölders of the regularized harmonic densities on the stages $n_c = 2$, 3, 4 and 5 of the cascade in figure 1. The $n_c = 5$ plot is marked with squares. The convergence is rapid, in the sense that the $n_c = 4$ and 5 plots are nearly identical. The $C_n(\alpha)$ is expected to converge ultimately to a smooth $\cap$-shaped curve $C(\alpha)$, which is identical to $f(\alpha) - D$, where $D = \ln 5/\ln 3$.

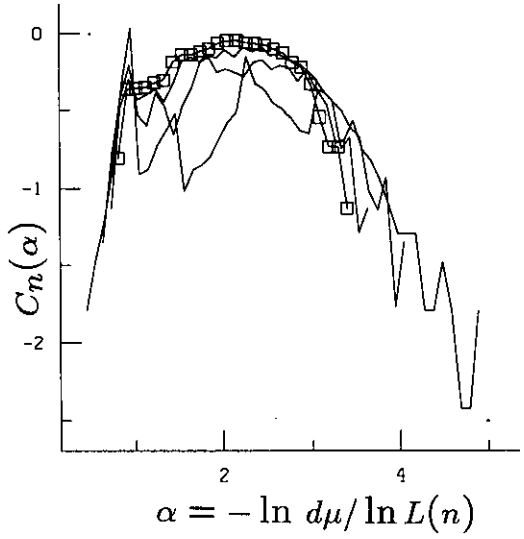

Figure 9. This is the same plot as in figure 8, except that the harmonic density is unregularized. The convergence is much less rapid. The maximum Hölder in the $n_c = 2$ stage is much larger than that of the more asymptotic state $n_c = 5$. This is due to an overarticulation of fold singularities, such as the one to the left of the symbol 0.14 in figure 1. This was avoided in figure 8 by using regularization.

An estimate of the regularized density on the boundary is obtained by first computing the electrostatic potential ϕ_i at the lattice nearest neighbours of the structure. Then the site probability $\mu(i) = \phi_i / \Sigma_j \phi_j$ is an estimate of the harmonic measure for that subset of size $\delta(n)$ of the boundary, which is a nearest neighbour of site i. Then the $\varepsilon = k\delta(n)$ regularized density $\mathrm{d}\mu_\varepsilon(i)$ at site i is

$$\mathrm{d}\mu_\varepsilon(i) = \frac{\sum_{j=i-k/2}^{i+k/2} \mu(j)}{\varepsilon}. \tag{4}$$

The normalized density-Hölders of this regularized density are defined as

$$\alpha_i(\varepsilon) = \frac{-\log \mathrm{d}\mu_\varepsilon(i)}{\log L(n)} = -\frac{1}{n} \log_3 \mathrm{d}\mu_\varepsilon(i). \tag{5}$$

The choice of ε is extremely important. This is very clearly illustrated by the Hölders of the harmonic measure on the first stage of the cascade shown in figures 2(*a*) or 5. The distribution of the corresponding Hölders, shown for finite δ in figure 6, is supposed to give information on the geometry of this stage. In the continuum limit $\delta \to 0$, without regularization (i.e. in the case $\varepsilon = \delta$), the densities at the four folds defining the square cavity will either approach 0 or ∞. Thus the distribution of the Hölders in figure 6 would be distorted by the singular contribution of these folds. At this stage it is the density at the centre bottom of the cavity that is related to its shape, and not the density in the lower-left or -right corner of the cavity. Their singular contributions to the densities of Hölders are easily removed by regularization. Appendix 2 describes an example of regularization for a needle-shaped boundary. The natural choice for the regularization parameter ε is the size of the smallest relevant geometric detail in the boundary. In the present case, that means $\varepsilon = 1$; i.e. $k = 1/\delta(n)$ in equation (4).

In figure 8, we show the Cramèr collapse [2, 10] of the probability densities $P_n(\alpha)\,\mathrm{d}\alpha$ of the Hölders for stages $n = 2$, 3, 4, 5, with $\varepsilon = 1$. The ordinate is $C_n(\alpha) = \ln P_n(\alpha)/\ln L(n)$. The harmonic measure on a linearly self-similar boundary is known to be a restricted multifractal [11-13], hence one expects $C_n(\alpha)$ to converge to a limit $C(\alpha) = f(\alpha) - 1$ as $n \to \infty$. This convergence is clearly visible in the figure.

In order to see the effect of the regularization, we have plotted in figure 9 the results for $\varepsilon = \delta$. The left-most and right-most tails are now distorted by the contributions of the unregularized local singularities at the folds.

Since the above analysis is based on the density, rather than on 'site probabilities', the results are independent of the lattice used to estimate the Laplacian potential. As has been demonstrated, different lattice constants can be used at different stages of the cascade, while allowing the results to be combined. Of course, this is only true as long as the lattice constants used are smaller than the smallest relevant length scale on each of the boundaries.

7. Random fractal boundaries and DLA

To facilitate the comparison of ***K*** with DLA it is best to interpret it in terms of growth as shown in figure 10. At each time step t, one bond of size 1 is added to both the left and right halves of the 'cluster'. The time steps $t_n = (5^n - 1)/2$ correspond to the different generations $n_c = n$ of the geometric cascade discussed in the previous sections. This process makes ***K*** 'grow' by the addition of bonds in the 'growth zone', which is the

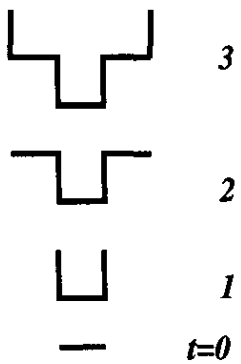

Figure 10. The first four stages of a growing version of the square Koch tree. At each subsequent time step a new bond is added to the left and right halves of the structure. *This is done in such a manner that the geometric cascade stages n_c of figure 1 are recovered* after $(5^{n_c}-1)/2$ time steps.

most outward (highest) region of the cluster. In that region, small fjords cluster in a hierarchical fashion, thereby creating increasingly larger fjords.

Let the age of a fjord x be $N-t_x$, where N is the number of time steps in the whole set (i.e. number of bonds divided by 2), and t_x is the aggregation time of the first-added bond defining fjord x. The fjord of largest Euclidean size is very old, but includes subfjords of a variety of ages.

This definition of age is also applicable to DLA, and establishes no relation between the age and size of fjords. One finds *young* small fjords in the growth region, and *old* small fjords decorating the deep interior of the largest fjords. Also, the nesting number of a fjord is not determined by either its age or size. Young small fjords in the growing zone and old small fjords at the bottom of large fjords may have the same small values of n_s. For any size not too close to the overall size of the complete boundary, fjords come with a variety of n_ss and ages.

With these notions it becomes clear that (except for extreme cases) the harmonic measure of a subset of $\boldsymbol{K}$ is not a simple function of its age, size or location. In the square Koch tree the absolute smallest harmonic density is located in the smallest fjord having the largest n_s. This fjord is the oldest, and is located at the bottom of the deepest fjord. On the other hand, the absolute largest harmonic density is associated with younger ages and $n_s=0$. This tendency of increasing spatial localization when going to extremes is, of course, typical of *deterministic* multiplicatively generated multifractal measures.

In DLA, the picture is very similar. The cluster grows almost exclusively by the addition of atoms at the outer unscreened regions, resulting in a hierarchy of fjords. However, the hierarchy is no longer strict. This is best illustrated by comparing the Laplacian tree in figure 2(*c*) with the one for cylindrical on-lattice DLA in figure 3 of [9]. Needless to say, the Laplacian tree of a DLA is not regular at all. Nevertheless, one can clearly distinguish an increasingly narrowing branched Laplacian tree structure, consisting of mainstreams of zebra stacks with near-parallel walls. It is obvious from the randomness of the DLA boundary and of the complementary Laplacian tree that an underlying multiplicative process would be genuinely *random*. The observation that a young fjord, for which the nesting number is small, can have the smallest harmonic density on the whole DLA boundary [9, 10, 21] implies that the multiplier distribution of the associated random multiplicative process used in modelling the measure should

be such that an interval having a large measure at some late stage of the growth cascade can, in just one stage, acquire a subinterval having the smallest measure on the whole support. Such a multiplier distribution seems to indeed apply to DLA [10, 11].

This study of the Laplacian potential field in interaction with the linearly self-similar Koch tree clarifies the applicability of the notions of multiplicative cascades and the Hölder α in the description, modelling and understanding of the multifractality of the harmonic measure on linearly self-similar boundaries. These concepts have always been featured in the theory of multifractals, but are given additional meaning in terms of the mathematics and physics of the specific problem at hand. There have been many attempts to apply the theory of multifractals to the harmonic measure on DLA boundaries. This paper does not pretend to have shown exactly how to transfer what was found for the Koch tree to DLA. Nor does it pretend to give any clues as to why DLA is fractal [17]. However, it should give a clue as to how the geometry of the DLA boundary gives rise to a multifractal harmonic measure.

Appendix 1. Smoothness of the regularized density

This appendix shows why the local Hölder associated with the regularized density of the harmonic measure in equation (3), is 1 everywhere. The reason is that the measure is non-atomic: there are no points on the boundary with positive harmonic measure. This insures that the regularized density is continuous, and that its integral is continuous and at least once differentiable. If we denote this integral $\int_t^{t+x} \mathrm{d}\mu_\varepsilon(t)$ by $I_t(x)$, then $\alpha(t)=1$ follows from $I_t(x) \approx xI_t'(0)$ for $x \ll 1$.

For a more detailed proof we use the following slightly modified definition of the regularized density, $\mathrm{d}\mu_\varepsilon(t)=\mu(t, t+\varepsilon)/\varepsilon$. The integral in the definition (equation (3)) of the local Hölder, $I(x) \equiv \int_0^x \mathrm{d}\mu_\varepsilon(t)$, can be rewritten as

$$I(x)=\frac{1}{\varepsilon}\int_0^x \mu(t, t+\varepsilon)\,\mathrm{d}t=\frac{1}{\varepsilon}\int_0^x \mu(t, x)\,\mathrm{d}t+\frac{x}{\varepsilon}\mu(x, \varepsilon)+\frac{1}{\varepsilon}\int_0^x \mu(\varepsilon, t+\varepsilon)\,\mathrm{d}t \tag{6}$$

for $x<\varepsilon$. So $(x/\varepsilon)\mu(x_u, \varepsilon) \leqslant I(x) \leqslant (x/\varepsilon)(\mu(0, x)+\mu(0, \varepsilon)+\mu(\varepsilon, \varepsilon+x))$. Where $x_u < \varepsilon$ is an arbitrary upper bound to x. Since the measure is non-atomic, the terms $\mu(0, x)$ and $\mu(\varepsilon, \varepsilon+x)$ can be made arbitrarily small with respect to $\mu(0, \varepsilon)$ for small enough x, and it follows that $\alpha(0)=1$. The result holds for all points of the boundary, since the origin is arbitrary.

Appendix 2. Regularizing the harmonic measure on a needle

The density of the harmonic measure on the half line $x \in [0, \infty)$ in the Euclidean plane has local Hölder 1 everywhere, except for the power law singularity of local Hölder $\alpha_{\min}=\frac{1}{2}$ at the origin $(0, 0)$. The density near the origin is of the form

$$\mathrm{d}\mu(x)=\alpha_{\min}L^{-\alpha_{\min}}x^{\alpha_{\min}-1}$$

where an upper cut-off L, the size of the needle, has been introduced. Thus the ε-regularized density $\mathrm{d}\mu_\varepsilon$ at x is

$$\mathrm{d}\mu_\varepsilon(x)=\frac{1}{\varepsilon}L^{-\alpha_{\min}}[(x+\varepsilon)^{\alpha_{\min}}-x^{\alpha_{\min}}].$$

Therefore, the normalized density-Hölder at the origin of the singularity is

$$\alpha_\varepsilon(0) = -\ln_L \mathrm{d}\mu_\varepsilon(0) = \alpha_{\min} + (1-\alpha_{\min})\frac{\ln \varepsilon}{\ln L}.$$

This shows that, in the absence of regularization, i.e. $\varepsilon = 0$, the Hölder would diverge, and the effect of increasing L would be invisible. For finite ε, the maximum Hölder $\alpha_\varepsilon(0)$ converges to $\alpha_{\min} = \frac{1}{2}$ for $L \to \infty$. It also follows that the speed of the convergence depends on ε.

Appendix 3. Equivalence of the density of α on congruent boundaries

In order to prove that $P'_{B'}(\alpha') = P_B(\alpha')$ in section 4.2, let us coarse grain both B and B' in figure 4 with segments of size ε and $\varepsilon' = \lambda\varepsilon$, respectively. The harmonic measure $\mu_\varepsilon(i)$ and $\mu'_{\varepsilon'}(i)$ of each of the corresponding segments on B and B' will differ by a factor λ: $\mu'_{\varepsilon'}(i) = \lambda\mu_\varepsilon(i)$. Therefore their coarse-grained densities are the same, i.e., $\mathrm{d}\mu'(i) = \mu'_{\varepsilon'}(i)/\varepsilon' = \lambda\mu_\varepsilon(i)/\varepsilon' = \mathrm{d}\mu(i)$, and thus are the coarse-grained density-Hölders $\alpha = -\log \mathrm{d}\mu_\varepsilon$ and $\alpha' = -\log \mathrm{d}\mu'_{\varepsilon'}$. Now, let $P_\varepsilon(\alpha)$ be the probability density of the Hölders α, i.e.

$$P_\varepsilon(\alpha)\,\mathrm{d}\alpha = \frac{N(\varepsilon, \alpha, \alpha+\mathrm{d}\alpha)}{\text{number of segments}} \tag{7}$$

where $N(\varepsilon, \alpha, \alpha+\mathrm{d}\alpha)$ is the number of segments of size ε with Hölders between α and $\alpha+\mathrm{d}\alpha$. (Note that, in the last paragraph of section 4.2, ε is equal to the lattice constant, and is not explicitly shown.) We then define $P_B(\alpha) = \lim_{\varepsilon\to 0} P_\varepsilon(\alpha)$. From a similar definition for B' it immediately follows that $P_\varepsilon(\alpha)\,\mathrm{d}\alpha = P'_{\lambda\varepsilon}(\alpha)\,\mathrm{d}\alpha$ and, therefore, $P'_{B'}(\alpha') = P_B(\alpha')$.

References

[1] Mandelbrot B B 1982 *The Fractal Geometry of Nature* (San Francisco: Freeman)
[2] Mandelbrot B B 1991 *Proc. R. Soc.* A **434** 97–8
[3] Witten T A and Sander L M 1981 *Phys. Rev. Lett.* **47** 1400
[4] Meakin P 1988 *Phase Transitions and Critical Phenomena* vol 12, ed C Domb and J Lebowitz (London: Academic) p 335
[5] Mandelbrot B B 1974 *J. Fluid Mech.* **62** 331
[6] Frisch U and Parisi G 1985 *Turbulence and Predictability of Geophysical Flows and Climate Dynamics, Proc. of the Enrico Fermi International School of Physics* ed M Ghil, R Benzi and G Parisi (New York: North-Holland) p 84
[7] Halsey T C, Jensen M H, Kadanoff L P, Procaccia I and Shraiman B I 1986 *Phys. Rev.* A **33** 1141
[8] Mandelbrot B B 1989 *Pure Appl. Geophys.* **131** 5 (also in Mandelbrot B B 1988 *Fluctuations and Pattern Formation (Cargèse, 1988)* ed H E Stanley and N Ostrowsky (Dordrecht: Kluwer) pp 345–60
[9] Mandelbrot B B and Evertsz C J G 1990 *Nature* **348** 143
[10] Mandelbrot B B and Evertsz C J G 1991 *Physica* **177A** 386
[11] Procaccia I and Zeitak R 1988 *Phys. Rev. Lett.* **60** 2511
[12] Bohr T, Cvitanović P and Jensen M H 1988 *Europhys. Lett.* **6** 445
[13] Mandelbrot B B and Vicsek T 1989 *J. Phys. A: Math. Gen.* **22** L377
[14] Mandelbrot B B 1990 *Physica* **168A** 95
[15] Mandelbrot B B, Evertsz C J G and Hayakawa Y 1990 *Phys. Rev.* A **42** 4528
[16] Nagatani T 1987 *J. Phys. A: Math. Gen.* **20** L381; 1987 *Phys. Rev.* A **36** 5812; 1987 *J. Phys. A: Math. Gen.* **20** L641; 1987 *J. Phys. A: Math. Gen.* **20** 6135

[17] Pietronero L, Erzan A and Evertsz C J G 1988 *Phys. Rev. Lett.* **61** 861; 1988 *Physica* **151A** 207
[18] Niemeyer L, Pietronero L and Wiesmann H J 1984 *Phys. Rev. Lett.* **52** 1033
[19] Pietronero L and Wiesmann H J 1984 *J. Stat. Phys.* **36** 909
[20] Evertsz C J G, Mandelbrot B B and Normant F 1991 *Physica* **177A** 589
[21] Evertsz C J G, Mandelbrot B B and Woog L 1992 Variability of the form and of the harmonic measure for small off-off-lattice DLA *Phys. Rev.* A in press
[22] Carleson L I and Jones P On coefficients of univalent functions and conformal dimension *Duke Math. J.* to appear
[23] Evertsz C J G, Jones P W and Mandelbrot B B 1991 *J. Phys. A: Math. Gen.* **24** 1889
[24] Kakutani S 1944 *Proc. Imp. Acad. Sci. (Tokyo)* **20** 706
[25] Evertsz C J G, Eskes H and Pietronero L 1989 *Europhys. Lett.* **10** 607